Int. J. Heat Mass Transfer. Vol. 35, No. 10, pp. 2695–2703, 1992
Printed in Great Britain

0017–9310/92 $5.00 + 0.00
Pergamon Press Ltd

Numerical simulation of surface tension- and combined buoyancy-driven convection in a liquid layer heated by a hot wire

J. MAQUET, G. GOUESBET and A. BERLEMONT

Laboratoire d'Energétique des Systèmes et Procédés, INSA de Rouen UA CNRS 230, 2, Place E. Blondel, BP 8, 76131 Mont-Saint-Aignan, France

(*Received* 20 *January* 1991 *and in final form* 29 *September* 1991)

Abstract—The characteristics of convection in liquid layers heated below the free surface are numerically studied. The mechanisms for convection are buoyancy and variation of surface tension with respect to temperature. Specific computations are performed to stress the influence of heat transfer at the interface and of interfacial viscosities. The transition between Marangoni and buoyancy regimes, when heating by an infinite hot wire located below the free surface, is investigated.

1. INTRODUCTION

THE ORIGINAL motivation of this work was to understand the instability mechanisms involved in thermal lens oscillations (or HBE: optical Heartbeat Experiments) observed in our laboratory (refs. [1–5], among others). In these experiments, a laser beam travels horizontally in a cell containing an absorbing liquid, near and below the free surface. When leaving the cell, the beam exhibits a strong divergence due to the well-known phenomenon of thermal lensing [6], and shows, when projected onto a screen, a regular and contrasted ring pattern. For some laser powers and wire–surface distances, the ring pattern may present unsteady behaviour (periodic, quasi-periodic, chaotic). These optical features are accompanied by oscillatory convection in the liquid bulk and oscillatory motion of the free surface.

To approach the understanding of these phenomena, a simpler experiment has been designed in which heating of the liquid is carried out by means of a hot wire located near and below the free surface (HWE: Hot Wire Experiments [7–9]). Critical frequencies and critical temperature differences at the onset of instability have been measured. In contrast with the case of HBEs which exhibit complex behaviour up to chaos, we only observed up to now one bifurcation from steady to oscillatory states in HWEs. This bifurcation is identified as being a supercritical Hopf bifurcation.

To theoretically explain and understand the aforementioned instability phenomena, three lines of research may be considered. In the first approach, we examined whether there could be any analogy between HBE/HWE and the case when an infinite horizontal liquid layer submitted to a vertical temperature gradient loses its stability through a Hopf bifurcation. References [10, 11] discuss this problem when two instability agencies, namely surface tension and buoyancy effects, are simultaneously taken into account. Reference [12] discusses the case when simultaneous shear effects are also present. Although these papers provide valuable results for the case of an infinite horizontal liquid layer submitted to a vertical temperature gradient in its own right, they are disappointing as far as the understanding of HBE/HWE is concerned. For instance, in the horizontal liquid layer case, overstability generically sets in only when the rigid wall is colder than the free surface. Conversely, in HBE/HWE, the free surface is colder than the liquid, suggesting that we are faced with a somewhat different nature of instability. In a second approach, we developed a simple model relying on a physical understanding of involved phenomena, dimensional analysis and concepts from the modern theory of non-linear dynamics [13–15]. According to this model, HBE/HWE instabilities would result from the coupling between a mechanical oscillator associated with the free surface and a thermal oscillator associated with the heat source. Although illuminating, this model necessarily introduces some degree of arbitrariness and, in any case, is unable to predict in detail all measured quantities. In the third line of research, we rely on numerical computations which are the only rigorous way to achieve full predictions of HBE and HWE data. This however leads to a numerical problem of tremendous complexity. In this paper, we report on a necessary first step, namely the computation of the basic convection state in HWE, prior to the onset of oscillatory behaviour.

Apart from our original motivation, a great interest is developed concerning combined buoyancy and thermocapillary flows. Various engineering systems such as crystal growth techniques, especially in low gravity environment [16], or glass manufacturing processes, incorporate buoyancy and surface tension

NOMENCLATURE

a_l	thermal diffusivity of the fluid	Vi	viscosity number
Bi	Biot number	v, w	velocity components
Bo	Bond number	y, z	Cartesian coordinates.
Cri	crispation number		
d_{hw}	distance between the hot wire and the free surface	Greek symbols	
		α_v	expansion factor of the fluid
g	gravity acceleration	δz_{f0}	free surface deformation
h	heat transfer coefficient at the free surface	δT_0	characteristic temperature difference
Gr	Grashof number	$\kappa+\varepsilon$	interfacial viscosities
Ma	Marangoni number	λ	thermal conductivity
p	pressure	ν	kinematic viscosity
Pr	Prandtl number	ρ	specific mass
t	time	σ	surface tension.
T	temperature		

mechanisms, warranting the practical interest of numerical computations such as the ones presented in this paper.

The paper is organised as follows. Section 2 is devoted to the mathematical formulation of the problem. Section 3 discusses the calculation procedure and reports on validations of our code against results published by de Vahl Davis [17], Bergmann and Ramadhyani [18], Kayser and Berg [19], and Napolitano *et al.* [20]. Section 4 discusses the influence of the heat transfer at the interface in the case of a square pool with a free surface and differentially heated sidewalls. The influence of interfacial viscosities under the circumstances is discussed in Section 5. Section 6 is devoted to the influence of coupling between buoyancy and Marangoni effects in the case of heating by a hot wire located below the free surface, this case being a direct consequence of our original motivation. Section 7 is a conclusion.

2. MATHEMATICAL FORMULATION

Several geometries can be studied by the computer code, but the case of greatest interest to us is the hot wire experiment. Therefore, notations are related to this case. The system (as shown in Fig. 1), consists of a pool of non-volatile liquid, with a horizontal line source of heat located below the free surface. The system is taken as infinite in the direction Ox parallel to the line heat source and is limited by rigid walls equidistant from the wire on both sides of it. The z-axis is vertically directed toward the free surface and Oy is the horizontal axis perpendicular to the wire. The values v and w are the horizontal and vertical velocity components. The subscript 1 is used for the liquid and 2 for the surrounding gas.

Due to the geometry, the liquid is assumed to be a 2D-Newtonian fluid. With the assumptions that the expansion factor $\alpha_v = -1/\rho_0 \partial\rho/\partial T$ and the temperature differences in the liquid are not too large, the Boussinesq–Oberbeck approximation applies [21]. With the distance d_{hw} between the hot wire and the free surface as a unit of length and d_{hw}^2/ν (ν, kinematic velocity) as a unit of time, the dimensionless governing equations, with dimensionless quantities indicated with the superscript symbol (+), read as follows.

Continuity equation

$$\frac{\partial v^+}{\partial y^+} + \frac{\partial w^+}{\partial z^+} = 0. \tag{1}$$

Momentum equations

$$\frac{\partial v^+}{\mathrm{d}t^+} + v^+\frac{\partial v^+}{\partial y^+} + w^+\frac{\partial v^+}{\partial z^+} = \Delta^+ v^+ - \frac{\partial p^+}{\partial y^+}$$

(horizontal component) (2)

$$\frac{\partial w^+}{\partial t^+} + v^+\frac{\partial w^+}{\partial y^+} + w^+\frac{\partial w^+}{\partial z^+} = \Delta^+ w^+ - \frac{\partial p^+}{\partial z^+} + Gr\,T^+$$

(vertical component). (3)

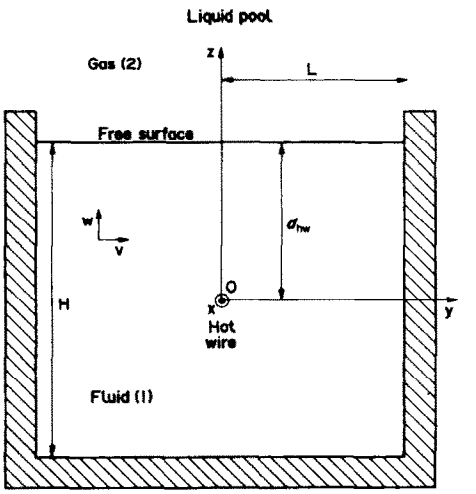

FIG. 1. Geometry of the problem.

Energy equation

$$\frac{\partial T^+}{\partial t^+}+v^+\frac{\Delta T^+}{\partial y^+}+w^+\frac{\Delta T^+}{\partial z^+}=\frac{\Delta^+ T^+}{Pr} \tag{4}$$

where p^+ is the reduced dimensionless pressure

$$p^+=[p_1-p_2-\rho_0 g(d_{hw}-z)]\frac{d_{hw}^2}{\rho_0 v^2} \tag{5}$$

and

$$T^+=\frac{T-T_0}{\delta T_0} \tag{6}$$

where T_0 is a reference temperature and δT_0 a characteristic temperature difference of the problem (difference between the hot wire and the temperature far above the free surface in the HWE-case).

Gr and Pr are the Grashof and Prandtl numbers defined by, respectively

$$Gr=\frac{g\alpha_v d_{hw}^3\delta T_0}{v^2},\quad Pr=\frac{v}{a_T} \tag{7}$$

in which a_T is the thermal diffusivity of the fluid.

Like Kayser and Berg [19], we assume that the free surface deformation δz_{fs} is small with respect to d_{hw}, then, for a stationary state, we have the kinematic condition $w^+=0$ at the free surface. Furthermore the free surface is assumed to be a 2D-Newtonian fluid with negligible mass. Following Aris [22], Scriven [23] and Scriven and Sternling [24], we obtain for the normal force balance at the free surface:

$$\frac{\partial^2(\delta z_{fs}^+)}{\partial y^{+2}}-Bo\cdot\delta z_{fs}=Cri\cdot Pr\left[-p^++2\frac{\partial w^+}{\partial z^+}\right] \tag{8}$$

and for the tangential force balance:

$$\frac{\partial v^+}{\partial z^+}-Vi\frac{\partial^2 v^+}{\partial y^{+2}}=-\frac{Ma}{Pr}\frac{\Delta T^+}{\partial y^+} \tag{9}$$

where Bo, Cri, Vi, Ma are the Bond, crispation, viscosity and Marangoni numbers defined by, respectively

$$Bo=\frac{\rho_0 g d_{hw}^2}{\sigma},\quad Cri=\frac{\rho_0 v a_T}{\sigma d_{hw}},$$

$$Vi=\frac{\kappa+\varepsilon}{\rho_0 v d_{hw}},\quad Ma=\frac{d\sigma}{dT}\frac{d_{hw}\delta T_0}{\rho_0\pi a_T} \tag{10}$$

in which σ is the surface tension of the interface and $(\kappa+\varepsilon)$ is the sum of the interfacial viscosities. For most fluids, surface tension decreases when temperature increases. Therefore Ma is usually negative when δT_0 is positive.

Another boundary condition is obtained by invoking the Newton heat transfer law at the free surface

$$\frac{\partial T^+}{\partial z^+}=-Bi\,T^+ \tag{11}$$

where Bi is the Biot number:

$$Bi=\frac{hd_{hw}}{\lambda} \tag{12}$$

in which h is the heat transfer coefficient at the free surface, and λ the thermal conductivity.

The other boundary conditions on the walls and on the wire take various forms, depending on the cases under study, such as: no-heat-flux or fixed temperature at the walls, fixed temperature or fixed heat-flux at the hot wire, no slip condition for the velocities at the walls.

3. MAIN FEATURE OF THE CALCULATION PROCEDURE

The bulk equations are solved on a rectangular mesh by the finite-domain method introduced by Patankar and Spalding [25]. The discretization of the bulk equations is obtained by integrating these equations over control volumes. As usual in this method, the scalar variables T, p and the components of the velocity are located at the nodes of rectangular staggered grids for a better approximation of the convective fluxes. A finite difference scheme performed the time discretization. The alternate direction method is used at each step of time.

The calculation procedure is derived from the SIMPLE algorithm [25]. At each step of time, temperature equation (4) and momentum equations (2), (3) are solved by using a tridiagonal matrix algorithm, then a pressure correction is obtained from the continuity equation (1). Iteration on time leads to the stationary state of convection. The deformation of the free surface is obtained at the end of computations from relation (8) expressed by a finite difference scheme.

Typical computational grids ranging from 25×25 to 50×50 are used, with finer spacing near the boundaries of the cavity. Computations were performed on SUN 3/60 workstations for the coarsest grids and on faster systems for the most refined ones.

Extensive verifications of our code were performed. The accuracy of the bulk equations solving was tested by comparing our results with the bench-mark numerical solution from de Vahl Davis [17]. In the case of natural convection in a square box with differentially heated side walls. Differences on all test quantities were within 3% of the bench-mark values for $Ra\leqslant 10^5$. This Ra value is higher than the values used for the other computations related in this paper. The second set of tests concerned the velocity condition (8). Cases with pure Marangoni convection or with combined buoyancy and Marangoni convection were investigated by Napolitano [20] or Bergmann and Ramadhyani [18]. We performed calculations in the same cases: rectangular or square liquid pools with differentially heated walls, with positive and negative Marangoni numbers, liquid pools with fixed temperature at the floor and insulated walls. The agreement between these authors and our results is very

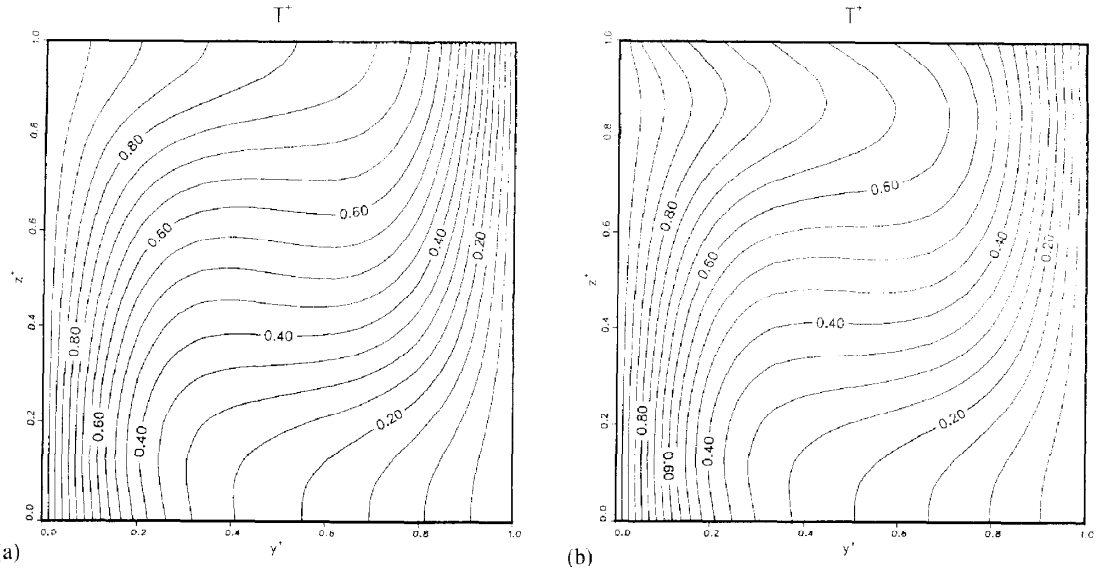

FIG. 2. Pure buoyancy convection. Isotherms (dimensionless temperature). (a) $Bi = 0$, (b) $Bi = 1$.

satisfactory (within 1% in all cases). One of the closest situations to ours is related by Kayser and Berg [19]. A liquid pool with insulated walls is heated by means of a power controlled line heat source which is, however, located along the bottom wall instead of being immerged in the liquid. They study, numerically and experimentally, the influence of the pool depth, of the heating rate, of the thermal expansivity, of the surface tension variations and of the heat transfer coefficient at the interface on the free surface deformation. We performed the same computations with the same results as Kayser and Berg. It strengthens our confidence for our computations in the HWE-case.

4. INFLUENCE OF THE HEAT TRANSFER AT THE FREE SURFACE

Heat transfer at the free surface is characterized by the Biot number (12). We checked the accuracy of our computer code with this thermal condition at the free surface, by comparing our results with those from the finite element code MODULEF [26] in pure conductive cases (motionless) in rectangular boxes with differentially heated sidewalls or with a hot wire located below a free surface.

To investigate the influence of an increasing Biot number, we performed computations for a square box with differentially heated sidewalls in three cases: a pure buoyancy-driven convection (Figs. 2 and 3), a combined buoyancy and Marangoni convection (Figs. 4 and 5) and a pure Marangoni flow (Figs. 6 and 7), starting in each situation from a simple case, without heat transfer at the free surface ($Bi = 0$, Figs. 2–7(a)), already studied by Bergman and Ramadhyani [18]. In Figs. 2–7 index 'a' corresponds to $Bi = 0$ and index 'b' to $Bi = 1$. In all cases, we have $Pr = 5$. In Figs. 2 and 3, we have $Gr = 2000$ and $Ma = 0$, in Figs. 4 and 5, $Gr = 2000$, $Ma = 1000$, in Figs. 6 and 7, $Gr = 0$, $Ma = -1000$. Bergman and Ramadhyani [18] used these values for Pr, Ma and Gr because they provide velocities of comparable intensity for pure buoyancy and for pure Marangoni flows. The left sidewall is the hot wall ($T^+ = 1$) and the right is cold ($T^+ = 0$). The dimensionless streamfunction is computed with a zero value at $y = 0$, $z = 0$.

As expected, the isotherms in case (b) are no longer orthogonal to the free surface and the flow intensity tends to decrease. This effect and the change in the shape of streamlines is more important for tension-driven flows than for buoyancy flows. We observed similar results when the liquid is heated by a hot wire.

5. INFLUENCE OF THE VISCOSITY NUMBER

The interfacial viscosities appear in equation (9) expressing the tangential force balance at the interface through the viscosity number Vi. Computations were performed in a square box with the same conditions as in Section 4, for a pure Marangoni flow ($Pr = 5$, $Ma = -1000$, $Gr = 0$) and with three viscosity numbers $Vi = 0$, 0.1, 1. The results for higher values of Vi are practically the same as for $Vi = 1$.

Except in the vicinity of the free surface, the influence of Vi on the flow remains very small and is not noticeable in buoyancy-driven flows. Figure 8 shows the influence of Vi on the free surface velocity v^+ vs y^+. The velocity peak near the cold wall decreases when increasing Vi. This fact was expected, because the term in relation (9) representing interfacial viscosities is proportional to the second tangential derivative of the surface velocity, that is to say the inverse of the curvature of the free surface velocity profile. Such an important curvature occurs only in a pure Marangoni flow at the top of the velocity peak near the cold wall.

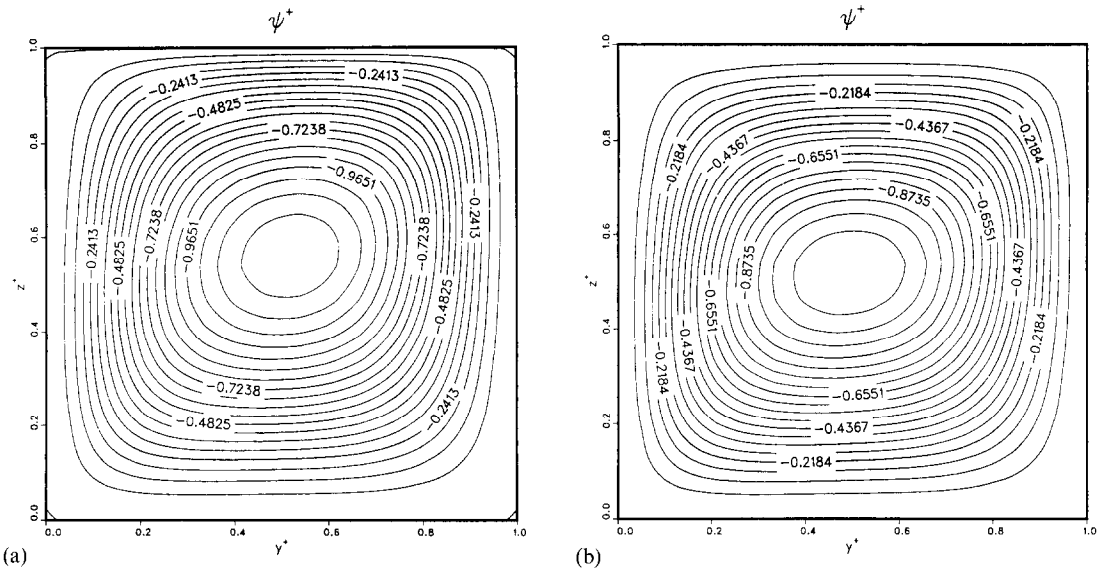

FIG. 3. Pure buoyancy convection. Dimensionless streamfunction. (a) $Bi = 0$, (b) $Bi = 1$.

6. LIQUID LAYER HEATED FROM A HOT WIRE

The case of a liquid heated by a hot wire lying at the floor of the pool has been experimentally and numerically studied by Kayser and Berg [19]. The system was limited by vertical thermally insulated walls and the wire is located in the middle of the floor. The rate of energy supplied from the line source is constant. Kayser and Berg show that a transition occurs in the concavity of the free surface deformation, depending on the depth of the liquid layer. Concave (depressed) profiles are produced in the shallower pools when the flow is dominated by surface tension gradients and convex (elevated) profiles in the deeper pools when the flow is dominated by buoyancy. They also show that the thermal expansivity α_v (occurring in Gr) and the temperature coefficient of surface tension $\partial\sigma/\partial T$ (occurring in Ma) are the primary determiners of the shape of the surface profile, while bulk viscosity and surface tension had only secondary effects. We performed computations in similar cases and our results are in agreement with Kayser and Berg.

The HWE-problem is slightly different. There the hot wire is no longer located on the floor of the pool, but at various distances between the floor and the free surface and its temperature is fixed. Another difference in our case is that the walls are at a fixed temperature. Computations were made for different liquids and depths of the hot wire in liquid pools of various dimensions. Concerning the influence of the

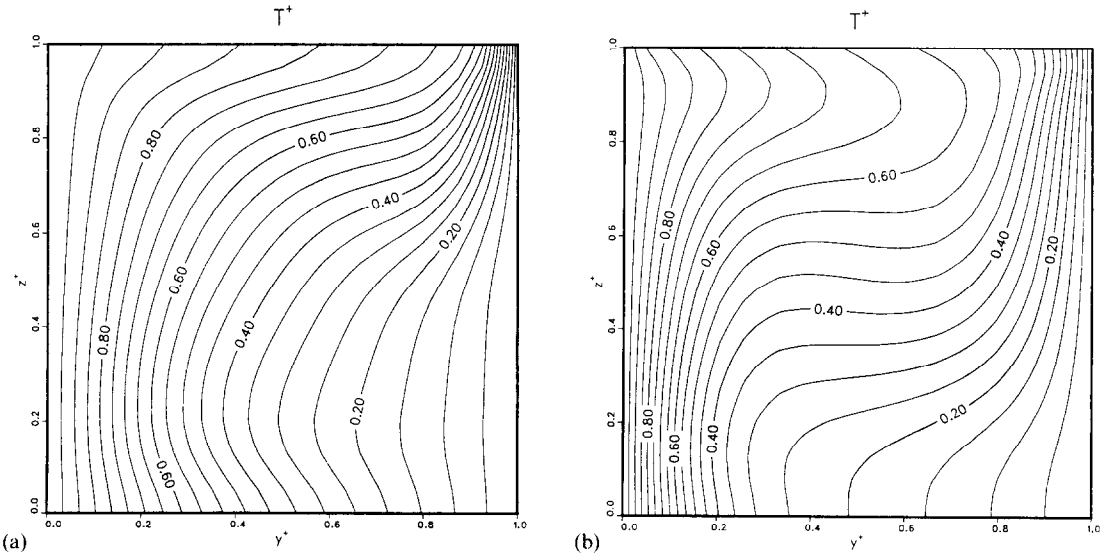

FIG. 4. Combined buoyancy and Marangoni convection. Isotherms (dimensionless temperature). (a) $Bi = 0$, (b) $Bi = 1$.

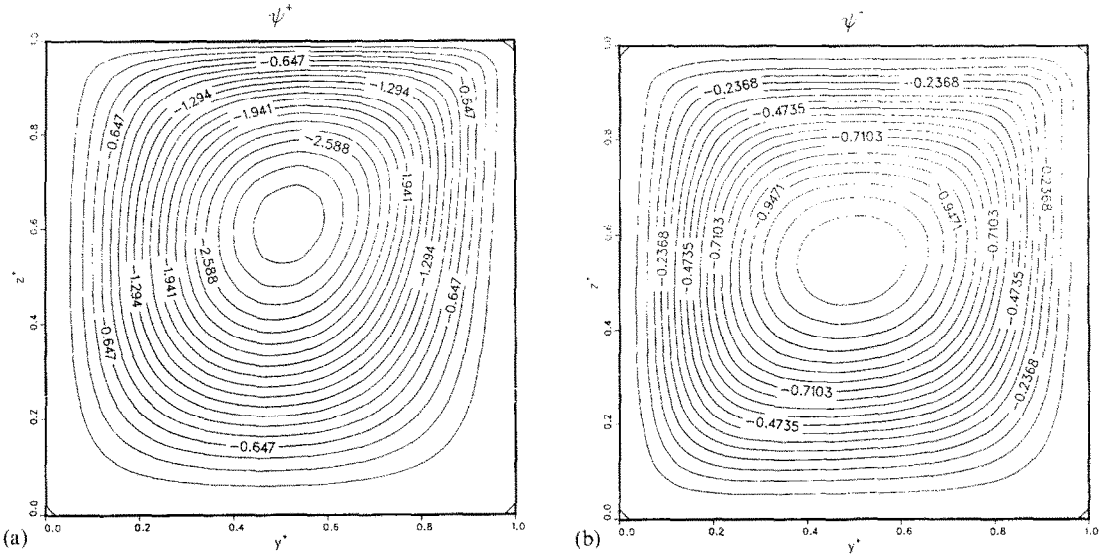

FIG. 5. Combined buoyancy and Marangoni convection. Dimensionless streamfunction. (a) $Bi = 0$, (b) $Bi = 1$.

thermophysical parameters, our conclusions are the same as Kayser and Berg's. We are showing here examples of computations concerning silicon oil (200 cs Dow-Corning Series) with the following thermophysical properties: at 20°C: $\rho = 971$ kg m^{-3}, $C_p = 1.484 \times 10^3$ J kg^{-1} K^{-1}, $\mu = 0.01942$ kg m^{-1} s^{-1}, $\lambda = 0.1546$ W m^{-1} K^{-1}, $\sigma = 21 \times 10^{-3}$ N m^{-1}, $d\sigma/dT = -69 \times 10^{-6}$ N m^{-1} K^{-1}, $\alpha_v = 0.37 \times 10^3$ K^{-1}. The temperature difference between the hot wire and the free surface is 0.1°C. The distance between the walls and the wire is four times the distance between the wire and the free surface.

We performed computations for $d = 1$ cm and $d_{hw} = 0.5$ cm. Figure 9 shows the isotherms for $d_{hw} = 1$ cm. Since the solutions are symmetric about the vertical centreline of the cavity, computations were performed only in the right half of the pool. The hot wire is located at $z^+ = 3.0$ at the left of the figure. The isotherms are not presented for $d_{hw} = 0.5$ cm, because they are not very different from the previous case, because the heat transfer in the layer is essentially due to the important viscosity of the fluid. Figure 10 shows the streamfunction for $d_{hw} = 1$ cm and Fig. 11 for $d_{hw} = 0.5$ cm. In the first case, we have essentially a buoyancy-driven flow with the streamlines approximately centred in the middle of the liquid pool. In the second case, we have a Marangoni-driven flow. As for the flow in a cavity with differentially heated sidewalls, the streamlines are concentrated near the free surface and near the cold wall with a peak in the free surface velocity. We find that, even for small temperature differences, the free surface deformation is not small

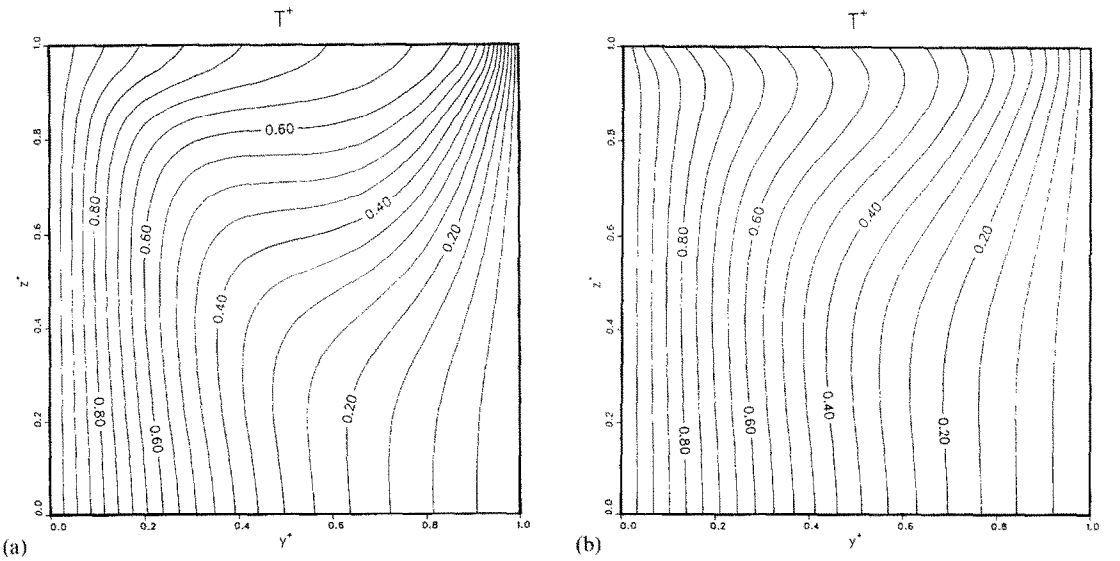

FIG. 6. Pure Marangoni convection. Isotherms (dimensionless temperature). (a) $Bi = 0$, (b) $Bi = 1$.

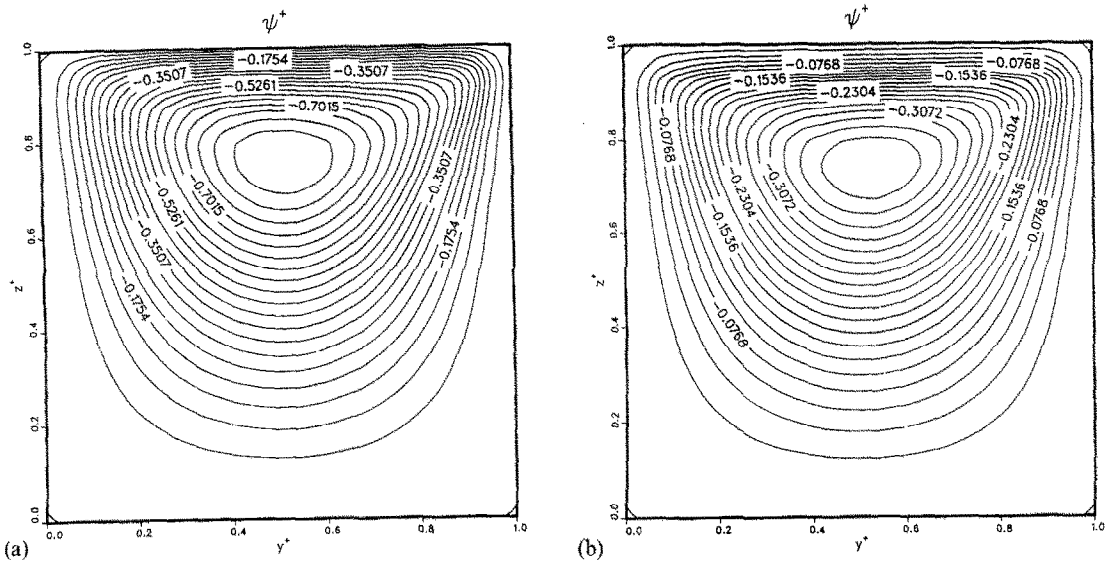

FIG. 7. Pure Marangoni convection. Dimensionless streamfunction. (a) $Bi = 0$, (b) $Bi = 1$.

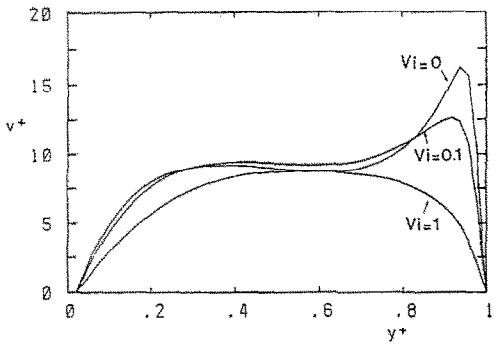

FIG. 8. Influence of the viscosity number on the free surface velocity. Dimensionless free surface velocity vs dimensionless distance.

with respect to d_{hw}, therefore relation (8) is no longer valid to obtain the surface profile in the case under study. We have to refine our model for the free surface to be in better agreement with experimental problems.

7. CONCLUSIONS

Combined buoyancy- and surface tension-driven flows have been simulated for a liquid layer with a free surface. Heat transfer at the free surface tends to decrease fluid velocity, especially for pure tension-driven flows. The influence of interfacial viscosities is only noticeable in the vicinity of the free surface and, in the most practical cases, is negligible. The computer code is now able to simulate the flow and the tem-

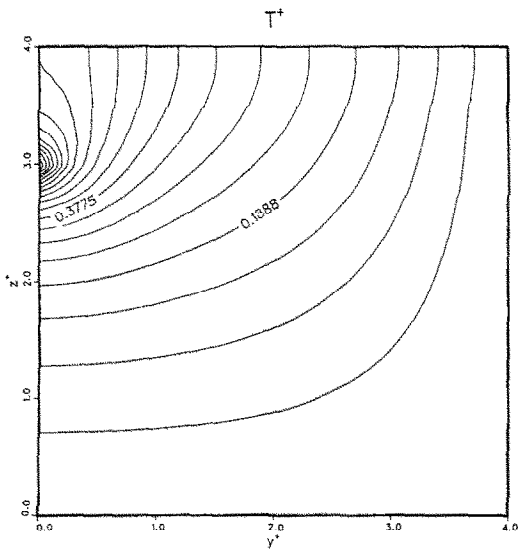

FIG. 9. Liquid pool heated from a hot wire. Isotherms (dimensionless temperature).

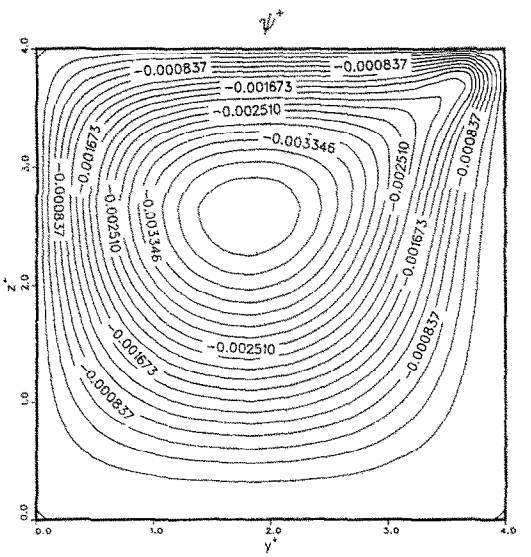

FIG. 10. Liquid pool heated from a hot wire, $d_{hw} = 1$ cm. Dimensionless streamfunction.

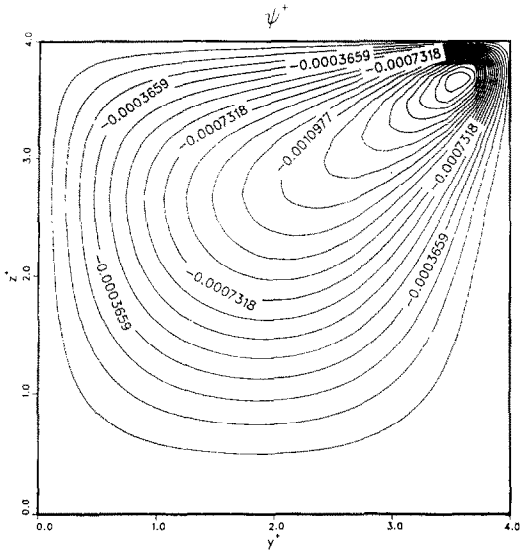

FIG. 11. Liquid pool heated from a hot wire, $d_{hw} = 0.5$ cm. Dimensionless streamfunction.

perature field in a liquid layer heated from a hot wire located at various distances from the free surface. An example of computations is presented for silicon oil, showing the transition between Marangoni and buoyancy regimes. However, more effort is required to predict instability characteristics observed in HWEs and HBEs. From that point of view, these experiments provide severe test-cases to assess the possibilities of more sophisticated codes devoted to the computations of surface tension- and buoyancy-driven flows.

REFERENCES

1. R. Anthore, P. Flament, G. Gouesbet, M. Rhazi and M. E. Weill, A note on interaction between a laser beam and some liquid media, *Appl. Optics* **21,** 2–4 (1982).
2. G. Gouesbet, M. Rhazi and M. E. Weill, A new heart-beating phenomenon, and the concept of 2D-optical turbulence, *Appl. Optics* **22,** 304–309 (1983).
3. G. Gouesbet, M. E. Weill and E. Lefort, Convective and free surface instabilities provoked by heating below an interface, *AIAA J.* **24,** 1234–1330 (1986).
4. G. Gouesbet and E. Lefort, Dynamical states and bifurcations of a thermal lens using spectral analysis, *Phys. Rev. A* **37,** 4903–4915 (1988).
5. G. Gouesbet, Oscillatory instabilities produced by laser or hot-wire heating below an interface, *Int. J. Japan Soc. Mech. Engrs* **32,** 301–308 (1989).
6. J. P. Gordon, R. C. C. Leite, R. S. Moore, S. P. S. Porto and J. R. Whinnery, Long-transient effects in lasers with inserted liquid samples, *J. Appl. Phys.* **36,** 3–8 (1984).
7. M. E. Weill, M. Rhazi et G. Gouesbet, Oscillations d'une surface libre chauffée sous l'interface à l'aide d'un fil, *C.R. Acad. Sci. Paris* **T294,** 567–570 (1982).
8. M. E. Weill, M. Rhazi and G. Gouesbet, Experimental investigation of oscillatory phenomena produced by a hot-wire located near and below a free surface, *J. Physique* **46,** 1501–1506 (1985).
9. G. Gouesbet, New presentation of experimental results for overstability phenomena produced by a hot-wire located near and below a free surface, *PhysicoChem. Hydrodyn.* **8,** 349–352 (1987).
10. G. Gouesbet and J. Maquet, Examination of an analogy toward the understanding of thermal lens oscillations, *AIAA J. Thermophys. Heat Transfer* **3,** 27–32 (1989).
11. G. Gouesbet, J. Maquet, C. Roze and R. Darrigo, Surface tension- and coupled buoyancy-driven convection instability in a horizontal liquid layer. Overstability and exchange of stability, *Physics Fluids* **2,** 903–911 (1990).
12. C. Roze, G. Gouesbet and J. Maquet, Overstability under simultaneous surface tension, buoyancy and shear effects in a horizontal liquid layer, 28th AIAA Aerospace Sciences Meeting, Reno, U.S.A., 8–11 January (1990).
13. G. Gouesbet and J. Maquet, A simple model to understand overstability in thermal lensing, *Int. Commun. Heat Mass Transfer* **16,** 133–141 (1989).
14. G. Gouesbet, Dynamical states and bifurcations in a new therm-dynamical nonlinear system: optical heartbeats and associated phenomena, *Entropie* No. 153/154, 47–61 (1990).
15. G. Gouesbet, Simple model for bifurcations ranging up to chaos in thermal lens oscillations and associated phenomena, *Phys. Rev. A* **42,** 5928–5945 (1990).
16. D. Schwabe, Marangoni effects in crystal growth melts, *PhysicoChem. Hydrodyn.* **2,** 263–280 (1981).
17. G. de Vahl Davis, Natural convection of air in a square cavity: a bench mark numerical solution, *Int. J. Numer. Meth. Fluids* **3,** 249–264 (1983).
18. T. L. Bergmann and S. Ramadhyani, Combined buoyancy- and thermocapillary-driven convection in open square cavities, *Numer. Heat Transfer* **9,** 441–451 (1986).
19. W. V. Kayser and J. C. Berg, Surface relief accompanying natural convection in liquid pools heated from below, *J. Fluid Mech.* **57,** 739–752 (1973).
20. L. G. Napolitano, C. Golia and A. Viviani, Numerical simulation of unsteady thermal Marangoni flows, *Proc. 5th European Symp. on Material Sciences under Microgravity*—Schloss Elmau, 5–7 November (1984).
21. H. Oertel, Jr, Thermal instabilities in convective transport and instability phenomena. In *Zierep and Oertel*, pp. 3–24. G. Braun, Karlsruhe (1982).
22. R. Aris, *Vectors and the Basic Equations of Fluid Mechanics*. Prentice Hall, Englewood Cliffs, New Jersey (1962).
23. L. E. Scriven, Dynamics of a fluid interface. Equation of motion for Newtonian surface fluids, *Chem. Engng Sci.* **12,** 98–108 (1960).
24. L. E. Scriven and C. V. Sternling, On cellular convection driven by surface tension gradients: effect of mean surface tension and surface viscosity, *J. Fluid Mech.* **19,** 321–340 (1964).
25. S. V. Patankar and D. B. Spalding, A calculation procedure for heat, mass and momentum transfer in three-dimensional parabolic flows, *Int. J. Heat Mass Transfer* **15,** 1787–1806 (1972).
26. The Club MODULEF: A library of computer procedures for finite element analysis, INRIA, Rocquencourt, France (1982).

SIMULATION NUMERIQUE D'UNE CONVECTION CONDUITE PAR LA TENSION INTERFACIALE ET LES FORCES DE FLOTTEMENT DANS UNE COUCHE LIQUIDE CHAUFFEE PAR UN FIL CHAUD

Résumé—On étudie numériquement les caractéristiques de la convection dans des couches liquides chauffées sous la surface libre. Les mécanismes de la convection sont le flottement et la variation de tension interfaciale vis-à-vis de la température. Des calculs spécifiques sont conduits pour connaître l'influence du transfert thermique à l'interface et des viscosités interfaciales. On étudie la transition entre les régimes de Marangoni et de flottement lorsque le chauffage est réalisé par un fil chaud infini logé sous la surface libre.

NUMERISCHE SIMULATION DER GEMISCHTEN OBERFLÄCHENSPANNUNGS- UND AUFTRIEBSINDUZIERTEN KONVEKTION IN EINER DURCH EINEN DRAHT BEHEIZTEN FLÜSSIGKEITSSCHICHT

Zusammenfassung—Die Eigenschaften der Konvektion in einer Flüssigkeitsschicht, die unterhalb der freien Oberfläche beheizt wird, werden numerisch untersucht. Die Konvektionsströmung wird durch Auftrieb und durch temperaturbedingte Unterschiede der Oberflächenspannung induziert. Besondere Berechnungen werden ausgeführt, um den Einfluß des Wärmeübergangs an der Grenzfläche und der Grenzflächenviskosität zu betonen. Zusätzlich wird der Übergang zwischen dem marangonigesteuerten und dem auftreibsgesteuerten Bereich für eine Beheizung durch einen unendlich langen Draht unterhalb der freien Oberfläche untersucht.

ЧИСЛЕННОЕ МОДЕЛИРОВАНИЕ КОНВЕКЦИИ ЗА СЧЕТ ПОВЕРХНОСТНОГО НАТЯЖЕНИЯ И ПОДЪЕМНЫХ СИЛ В ЖИДКОМ СЛОЕ, НАГРЕВАЕМОМ ПРОВОЛОКОЙ

Аннотация—Численно исследуются характеристики конвекции в жидких слоях с нагреваемой снизу свободной поверхностью. Конвекция обусловлена подъемными силами и изменением поверхностного натяжения с температурой. Проводятся расчеты с целью установления влияния теплопереноса и вязкостей на границе раздела. Исследуется переход между режимом Марангони и течением, обусловленным подъемными силами при нагреве бесконечной проволокой, расположенной под свободной поверхностью.